V. RADIO ASTRONOMY*

Academic and Research Staff

Prof. A. H. Barrett
Prof. B. F. Burke
Prof. L. B. Lenoir
Prof. D. H. Staelin
Dr. S. H. Zisk
J. W. Barrett
Patricia P. Crowther
P. L. Seymour

Graduate Students

M. S. Ewing
N. E. Gaut
M. Melnick
J. M. Moran, Jr.
G. D. Papadopulos
E. C. Reifenstein III
A. E. E. Rogers
R. M. Weigand
T. L. Wilson

A. 20-CHANNEL MICROWAVE SPECTROMETER

A new multichannel microwave radiometer has been constructed for studying spectral lines of 4-40 Mc/sec width. The system operates, at present, near 23.86 GHz, a resonance frequency of O_3. The system is basically a superheterodyne Dicke radiometer with IF frequency 20-100 MHz. The output of the IF amplifier is filtered into 20 adjacent channels, 4-MHz wide. Each channel output is then processed separately. There is no image rejection. A block diagram is shown in Fig. V-1.

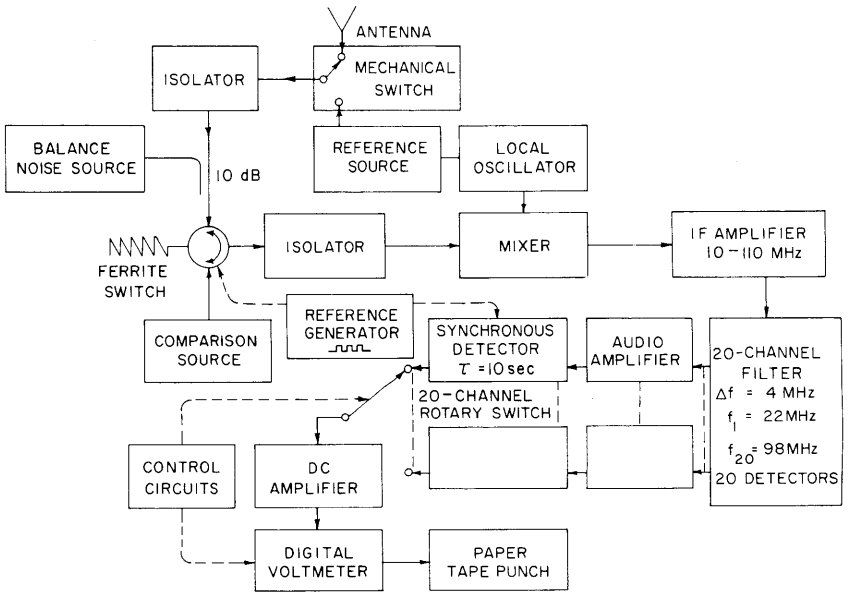

Fig. V-1. 20-channel microwave radiometer.

*This work was supported principally by the National Aeronautics and Space Administration (Grant NsG-419 and Contract NSR-22-009-120); and in part by the Joint Services Electronics Programs (U.S. Army, U.S. Navy, and U.S. Air Force, Under Contract DA 28-043-AMC-02536(E), the U.S. Navy (Office of Naval Research) under Contract N00014-67-A-0204-0009, and the National Science Foundation (Grant GP-7046).

The system performance is limited principally by the noise figure of the mixer-preamplifier. This noise figure appears to be approximately 10 dB at the low IF frequencies, and 13 dB at the high frequencies. The system noise figure is approximately 3 dB greater, because of losses in the ferrite switch, isolators, and other waveguide components. The system ΔT_{rms} is approximately 1-2°K for a 10-sec integration time.

The spectral properties of the ferrite switch also limit the system performance. The ferrite-switch transfer function is different for the antenna and reference signals, and both of these transfer functions have spectral features of less than 100 MHz width. If the observed source is intense like the sun, then the ferrite switch contributes a large frequency-dependent signal to the total observed spectrum. This large signal now exceeds the desired dynamic range of the instrument for solar observations. Only less intense signals are now readily observed.

The 20-channel radiometer is quite flexible and can be adapted for use at other frequencies. The system will be useful for studies of the atmospheres of Earth and other planets and for laboratory studies of various microwave resonances.

D. H. Staelin, R. M. Weigand, J. M. Waters

B. RADIOMETRIC DETECTION OF ATMOSPHERIC OZONE

The 20-channel radiometer described in Sec. V-A has been used for the detection of the 19,2 → 18,3 line of atmospheric ozone (O_3) at a frequency of 23,860 MHz. The observations were conducted with a microwave horn viewing the atmosphere at zenith angles of 10° and 78°. Thus the line was seen in emission. Attempts to detect the line in absorption with the sun used as a background source were not attempted because the spectral properties of the microwave components at the radiometer input gave spectral responses that exceeded the dynamic range of the radiometer.

Preliminary observations, made during the week of May 1, 1967, revealed a spectral line at 23,860 MHz of 0.3°K amplitude at zenith angle 78°. The full linewidth at half maximum was approximately 10 MHz. A portion of this width results from averaging the data of adjacent frequency channels. At a zenith angle of 10° the line amplitude is approximately 0.1°K. The line intensities are in good agreement with that computed from a model of atmospheric ozone distribution.

Further observations and equipment modification are in progress.

A. H. Barrett, R. W. Neal, D. H. Staelin, R. M. Weigand

C. CALIBRATION SOURCE FOR A MICROWAVE RADIOMETER

This calibration device[1] consists basically of a waveguide termination, which is kept at a constant cool temperature by thermoelectric heat pumps. These pumps are

controlled by a switching circuit utilizing pulsewidth modulation to attain a DC-DC power conversion efficiency of 79% for the greatest temperature gradient of $\Delta T = 46°K$ across the thermoelectric pumps. To maintain this gradient a total power of 30 watts is drawn from the power supply. The thermoelectric heat pump has been used at ambient temperatures of 6°-36°. The corresponding coolest temperatures achievable were -40C and -20° C.

To achieve a constant temperature on the waveguide termination with an error of less than 0.1°C for an ambient temperature change of 30°C, the temperature on the waveguide is sensed by a thermistor. The switching circuit is controlled by using a thermistor bridge. By increasing the forward loop gain of this circuit to approximately 700, the error measured within the operational region of this device was less than 0.1°C for a 30°C change in ambient temperature. Taking into consideration steady-state errors attributable to the construction of the waveguide termination, we conclude that this device allows power calibration that is accurate within a total error of 0.5°C.

L. P. A. Henckels, W. B. Lenoir

References

1. Lutz Henckels, "Calibration Device for a Microwave Radiometer," S.B. Thesis, Department of Electrical Engineering, M.I.T., June 1967.

D. INFERENCE OF THE ATMOSPHERIC TEMPERATURE PROFILE FROM SIMULATED MICROWAVE MEASUREMENTS FROM SPACE

Recently, several authors[1-4] have discussed the inversion problem as it relates to the indirect measurement of atmospheric profiles (temperature, density, etc.) from satellites. These discussions are, in general, quite detailed, but, with one exception,[1] they present no analysis of the effect of measurement noise. Several of them also employ a data-smoothing technique to make a stable inversion more likely.

The work reported on here approaches the problem from a simpler point of view and achieves good results. Essentially, the goal is to make microwave measurements from a satellite and to infer the atmospheric temperature profile from 10 km to 60 km on the basis of these measurements. The effect of measurement error is to be included in the analysis. A point of departure from other methods is that rather than taking a given distribution of weighting functions[5] the weighting function distribution will be chosen to achieve the best results.

If we assume that N brightness temperature measurements are made from space, then the problem is to infer the atmospheric temperature profile on the basis of these measurements. The true brightness temperatures would be given by

$$T_{B_i} = \int_0^{h_s} T(h)\, WF_i(h)\, dh; \qquad i = 1, 2, \ldots N, \tag{1a}$$

with the weighting function defined by

$$WF_i(h) = \alpha[T(h), p(h), \nu_i] \exp\left(-\int_h^{h_s} \alpha[T(x), p(x), \nu_i]\, dx\right), \tag{1b}$$

where h_s is the satellite height, T(h) the desired temperature profile, p(h) the pressure profile, ν_i the frequency at which the measurement is made, and α the absorption coefficient of the atmosphere.

The temperature profile is approximated as

$$T(h) \sim f_o(h) + \sum_{j=1}^{N} a_j f_j(h), \tag{2}$$

(Note: in future relations the summation convention, with the summation symbol omitted, will be used) where the f's are functions chosen at the start and the a's are coefficients to be determined. Thus if the measurements were noiseless, Eq. 1a would be approximated by

$$T_{B_i} - \int_0^{h_s} f_o(h)\, WF_i(h)\, dh = a_j \int_0^{h_s} f_j(h)\, WF_i(h)\, dh, \tag{3}$$

which represents N linear equations with N unknowns, under the assumption that the weighting functions are known. To simplify the notation, let the left side of Eq. 3 be T'_{B_i}, and the coefficient of a_j on the right side be M_{ij}. Then Eq. 3 becomes

$$T'_{B_i} = M_{ij} a_j. \tag{4}$$

Thus the a's, if the inverse of the matrix M exists, are found to be

$$a_j = (M^{-1})_{jk}\, T'_{B_k}, \tag{5}$$

and the inferred profile is

$$T(h) = f_o(h) + (M^{-1})_{jk}\, T'_{B_k} f_j(h). \tag{6}$$

In practice, this would be accomplished by using a model atmosphere to compute the WF's and then inverting. The inversion result would be used to compute new WF's, and the inversion would be repeated to yield a new profile. This would be continued until a self-consistent result is obtained or until a divergence is evident. In fact, it is found that the WF's depend weakly on the temperature so that the procedure above converges rapidly to a self-consistent result, except when the WF's are so closely spaced that the

matrix, M, is almost singular.

To include the effects of noise in the analysis above it is necessary to replace T_{B_i} $\left(\text{or } T'_{B_1}\right)$ with $T_{B_i} + \delta T_{B_i}$ $\left(\text{or } T'_{B_i} + \delta T_{B_i}\right)$, where δT_{B_i} is the measurement error of i^{th} channel. When this is done the inferred profile is given by

$$T(h) = f_o(h) + (M^{-1})_{jk}\, T'_{B_k} f_j(h) + (M^{-1})_{jk}\, f_j(h)\, \delta T_{B_k}, \tag{7}$$

which is the noiseless inversion (Eq. 6) plus the effect of the noise.

In describing the following inversions, two error criteria will be followed. The first is the difference of the true profile and the noiseless inversion, defined by

$$\Delta T(h) = T(h) - f_o(h) - (M^{-1})_{jk}\, f_j(h)\, T'_{B_k}. \tag{8}$$

The second criteria is the rms deviation of the inversion of noisy measurements from the noiseless inversion as a function of height,

$$\delta T(h) = \left[\left\{\overline{(M^{-1})_{jk} f_j(h)\, \delta T^2_{B_k}}\right\}\right]^{1/2}, \tag{9}$$

where the bar over the squared quantity means an ensemble average. When individual channel noises are assumed to be independent and to have equal rms values of $\Delta T_{B_{rms}}$, Eq. 9 simplifies to

$$\delta T(h) = \left[(M^{-1})_{jk} f_j(h) (M^{-1})_{lk} f_l(h)\right]^{1/2} \Delta T_{B_{rms}}. \tag{10}$$

From Eq. 10 we can define a noise amplification factor, N(h), as

$$N(h) = \left[(M^{-1})_{jk} f_j(h) (M^{-1})_{lk} f_l(h)\right]^{1/2}. \tag{11}$$

Also of interest will be these two error criteria averaged over the height range for which the inversion is considered valid,

$$\Delta T = \left[\left\langle T(h)^2 \right\rangle\right]^{1/2} \tag{12a}$$

and

$$N = \left[\left\langle N(h)^2 \right\rangle\right]^{1/2}. \tag{12b}$$

Because of the very weak dependence of the WF on the temperature profile, an iterative procedure to correct the WF for the different profiles was not used. We assumed

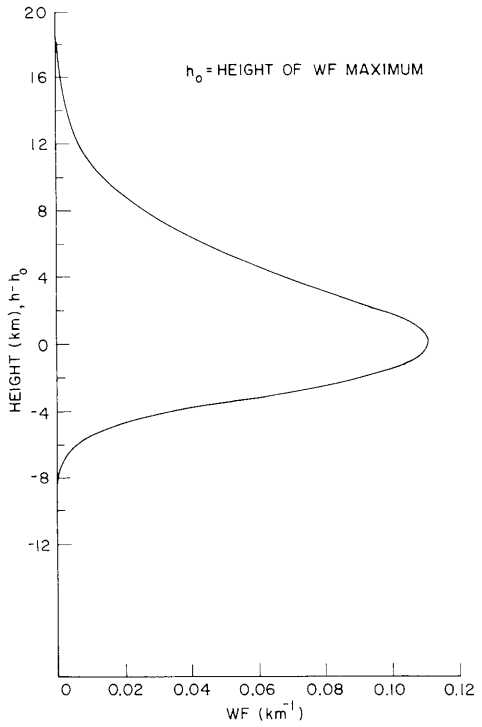

Fig. V-2. Typical weighting function.

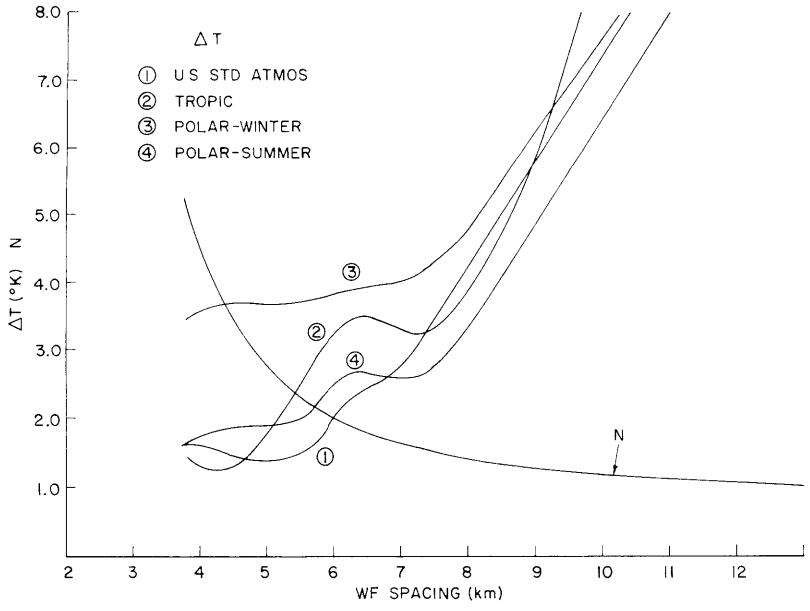

Fig. V-3. Error criteria for WF expansion.

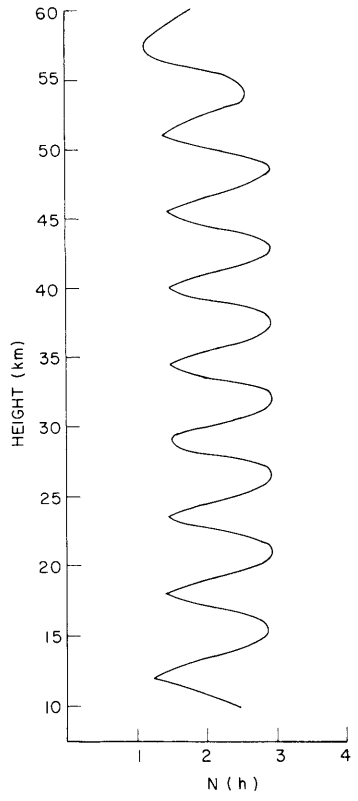

Fig. V-4.
N(h) for WF expansion with 5.5-km spacing.

that the WF's were independent of the temperature profile. A typical WF, shown in Fig. V-2, was used throughout. A WF was centered at 10 km and one at 60 km with from 2 to 12 others spaced uniformly between these heights. The goal was to infer the thermal profile from 10 km to 60 km which would require mapping two lapse rate reversals, the tropopause near 15 km and the stratopause near 50 km. Each inversion was done for 4 different model atmospheres: the 1962 U.S. Standard Atmosphere, a typical tropical atmosphere, a typical polar winter atmosphere, and a typical polar summer atmosphere.

The first set of inversions used the following functions to build the profile:

$$f_o(h) = 300 - 1.111\,h \tag{13a}$$

$$f_j(h) = WF_j(h). \tag{13b}$$

The zero-order function is used to give the profile the correct trends outside the valid height range, that is, increasing below 10 km and decreasing above 60 km. The choice of the WF's is based on several considerations; first, the noiseless inversion automatically yields the best rms error for these functions; second, measurement errors affect the profile mainly in the vicinity of the appropriate WF. Inversions were made for all 4 atmospheres with 4, 5, ... 13, 14 WF's spaced uniformly from 10 km to 60 km. The resulting inversion error criterion, ΔT, and the noise amplification, N, are plotted in Fig. V-3 against the WF spacing. As would be expected, the inversion error is best when the WF's are spaced closely while the noise amplification is greatest here.

If a measurement noise of $\Delta T_{B_{rms}} = 1°K$ is assumed, then a minimum total rms error is achieved for a spacing of ~5.5 km between adjacent WF peaks. This corresponds to a total of 10 WF's. N(h) for this choice is shown in Fig. V-4. Of the four inversions with this spacing, the best noiseless inversion and the worst are shown in Fig. V-5.

A second set of inversions was computed by using

$$f_o(h) = 300 - 1.111\,h \tag{14a}$$

$$f_j(h) = h^j(h-90), \tag{14b}$$

which is essentially just a polynomial expansion with the correct trends guaranteed outside the 10-60 km height range.

The resulting ΔT and N for various spacings are shown in Fig. V-6. For all spacings N is larger than it was for the WF expansion (Fig. V-3). The inversion error, ΔT, is, in general, smaller, however, and allows the use of fewer WF's.

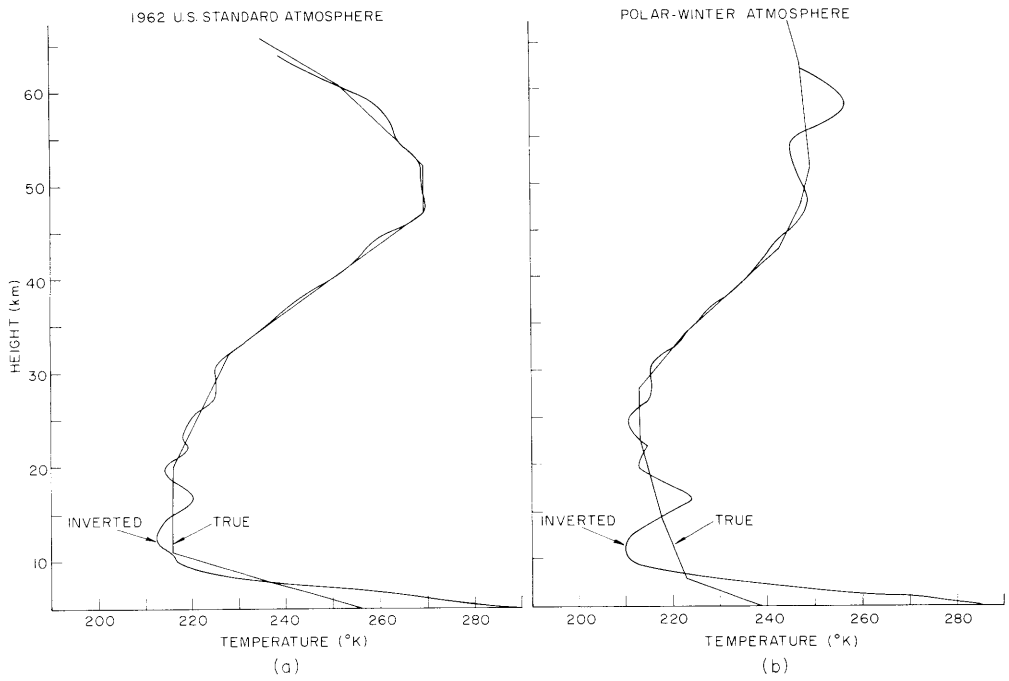

Fig. V-5. (a) Best inversion for WF expansion.
(b) Worst inversion for WF expansion.

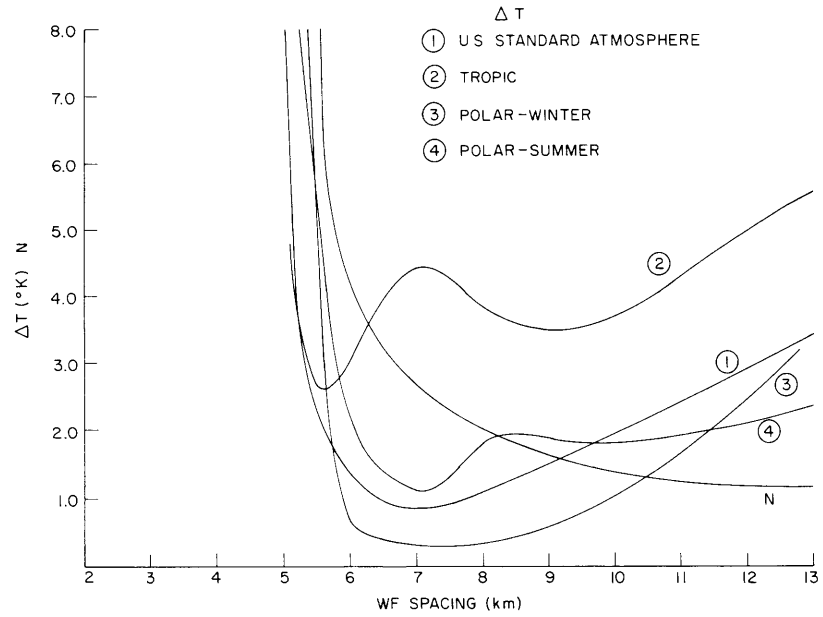

Fig. V-6. Error criteria for polynomial expansion.

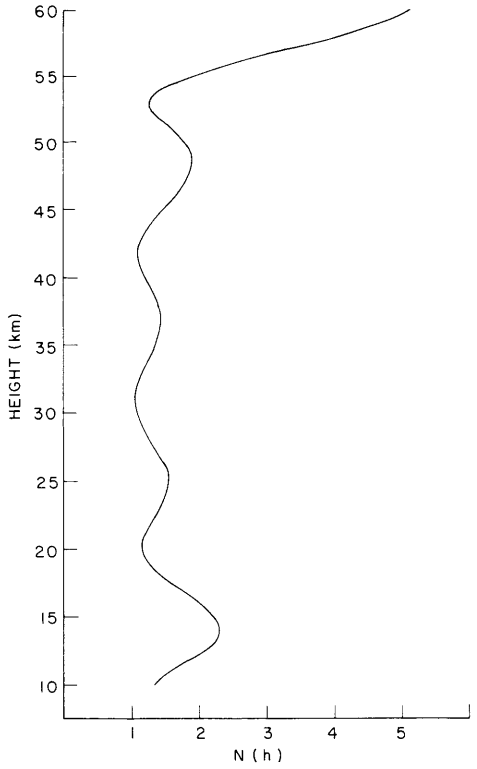

Fig. V-7.
N(h) for polynomial expansion with 8.35-km spacing.

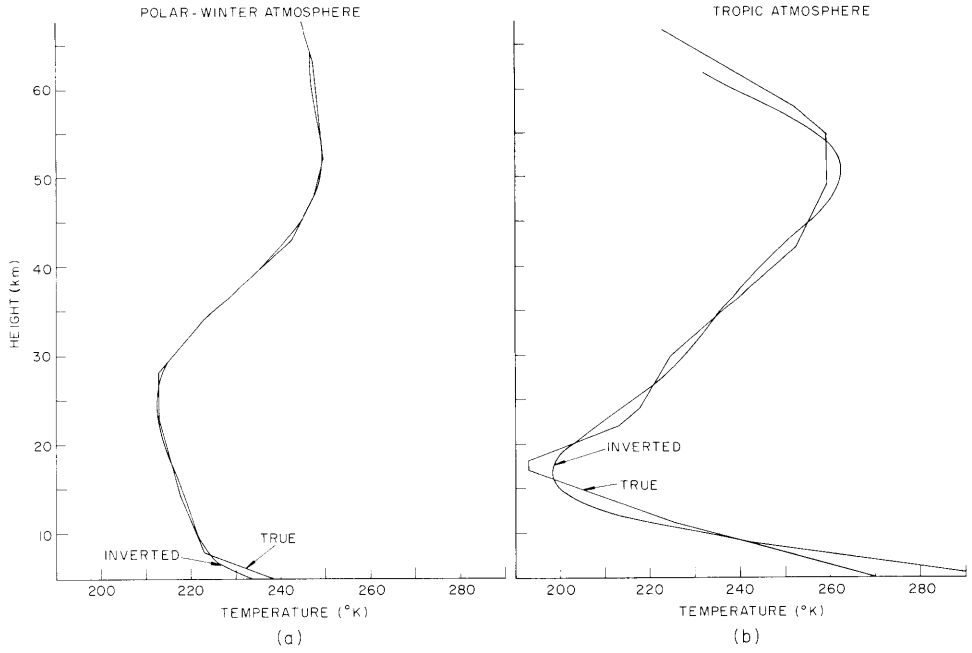

Fig. V-8. (a) Best inversion for polynomial expansion.
(b) Worst inversion for polynomial expansion.

At a spacing of ~5.5 km everything appears to blow up. This is partly due to the inversion itself which does not choose the coefficients to minimize the rms error (as the WF's do).

For $\Delta T_{B_{rms}}$ = 1°K the optimum spacing is ~8.35 km for a total of 7 WF's. In spite of employing fewer WF's, this choice results in a lower total error than the previous inversions. A noiser set of measurements would quickly change the picture. N(h) for the optimum spacing is shown in Fig. V-7. The best and worst inversions for this WF spacing are shown in Fig. V-8.

It appears that the polynomial expansion is better than the WF expansion because it does a better job and does not introduce the false wiggles that the WF's do. A potentially interesting expansion would be in terms of characteristic patterns[1] of the atmosphere. This, however, requires a statistical analysis of very many sample profiles, which makes it too time-consuming for us to investigate at this time.

W. B. Lenoir, R. F. Koehler, Jr.

References

1. C. D. Rogers, "Satellite Infrared Radiometer, A Discussion of Inversion Methods," Memorandum No. 66.13, Oxford University, September 1966.
2. S. Twomey, "Indirect Measurements of Atmospheric Temperature Profiles from Satellites: II Mathematical Aspects of the Inversion Problem," Mon. Weather Rev. 94 (6), 363-366 (June 1966).
3. D. H. Staelin, "Interpretation of Spectral Data," Quarterly Progress Report No. 85, Research Laboratory of Electronics, Massachusetts Institute of Technology, April 15, 1967, pp. 15-16.
4. N. E. Gaut, A. H. Barrett, and D. H. Staelin, "Results Obtained from the Inversion of Simulated Atmospheric Water-Vapor Spectra," Quarterly Progress Report No. 85, Research Laboratory of Electronics, Massachusetts Institute of Technology, April 15, 1967, pp. 16-19.
5. A. H. Barrett, J. W. Kuiper, and W. B. Lenoir, "Observations of Microwave Emission by Molecular Oxygen in the Terrestrial Atmosphere," J. Geophys. Res. 71, 4723-4734 (October 15, 1966).

E. REPORT ON THE H-109 ALPHA LINE SURVEY

The excited hydrogen lines allow one to observe the velocities of distant galactic H II regions. Assuming that the H I rotation curve applies to H II regions, one can find the distances of the sources from the sun, subject to certain ambiguities. One can then find the distribution of H II regions as a function of distance from the sun. Apart from this general galactic structure, the line may be helpful in unraveling the physics of certain special regions, such as Cygnus X and the Galactic Center. The linewidths and line intensities yield an estimate of electron temperatures. These, together with the angular sizes, continuum temperatures, and distances to the sources, give the linear size,

density, and mass of the individual H II regions.

We have recently completed a one-month survey in which the H-109 alpha line was observed at 5009 MHz, using the National Radio Astronomy Observatory's 140-ft telescope. The cooled parametric amplifier radiometer had a 70°K system temperature. This was frequency switched to a comparison band 2.4 MHz below the signal band. The frequency analysis was done with the Harvard 21-channel filter-bank receiver, which consists of a series of double-tuned filters providing channels spaced at 100 kHz, 1-db point to 1-db point. The rms temperature fluctuation for a 5 min on-off sequence was 0.05°K. We have observed 80 sources and definitely found the line in 52. Fifteen of 21 sources in Cygnus X, three of 8 in the Galactic Center, and forty-two of 52 in the rest of the galaxy have the line. The first data reduction involved drawing the curves by eye through the data points and measuring the relevant parameters.

Table V-1. Comparison of results.

	THIS SURVEY		MEZGER PAPER II	
SOURCE	LINE VLSR	$T_L \Delta V$	LINE VLSR	$T_L \Delta V$
W22	-5.2 km/s	512	-1.2 km/s	438
G353.2+0.9				
W22	-3.7	408	-5.9	722
G353.2+0.7				
M 8	4.9	190	3.5	274
W31	14.6	367	10.8	355
M16	25.1	131	27.9	135
M17	17.6	2970	17.6	2500
G15.0-0.7				
W43	92.4	586	88.6	701
W49A	9.4	294	7.4	316
W51	63.9	175	66.4	104
G49.0-0.3				
G49.5-0.4	58.0	635	59.1	945

First, we compare our data with those of Mezger and Hoglund.[1] Except for sources in Galactic Center, we have 10 sources for which both groups found the line. The results are listed in Table V-1.

Since the filters used by the two groups were different, the comparison of line strength must be made through the total line energy, $T_L \Delta\nu_L$. Although the line V_{lsr} agree rather well, the $T_L \Delta\nu_L$ values differ by as much as 50 per cent. The differences are not systematic and might be due, in part, to the calibration problems mentioned by Mezger in Paper II.

The main effort is directed toward constructing a distribution of H II regions in the galaxy. Therefore we restrict our attention to the region between L = 6° and L = 50°, examining only the velocity distribution of the lines. We assume that the H II regions obey the H I rotation curve and take our distance-velocity relation from Schmidt's galactic model.[2] For sources located inside R = 10 kpc, there are two possible distances from the sun. The reason for this is that a line drawn through a circle will cut the circle in two points. For the 10 sources previously treated by Mezger, we have adopted his choice of distance. For the remaining sources, we have adopted 3 criteria. If the source is more than 0.5° out of the plane, the continuum measurements indicate an extended source, and the source's line radiation is strong, say, T_l = 0.15°K or more, the source is nearby. The results are shown in Fig. V-9. We find that sources with weaker line emission are more distant. Thus by looking at the very weak sources in

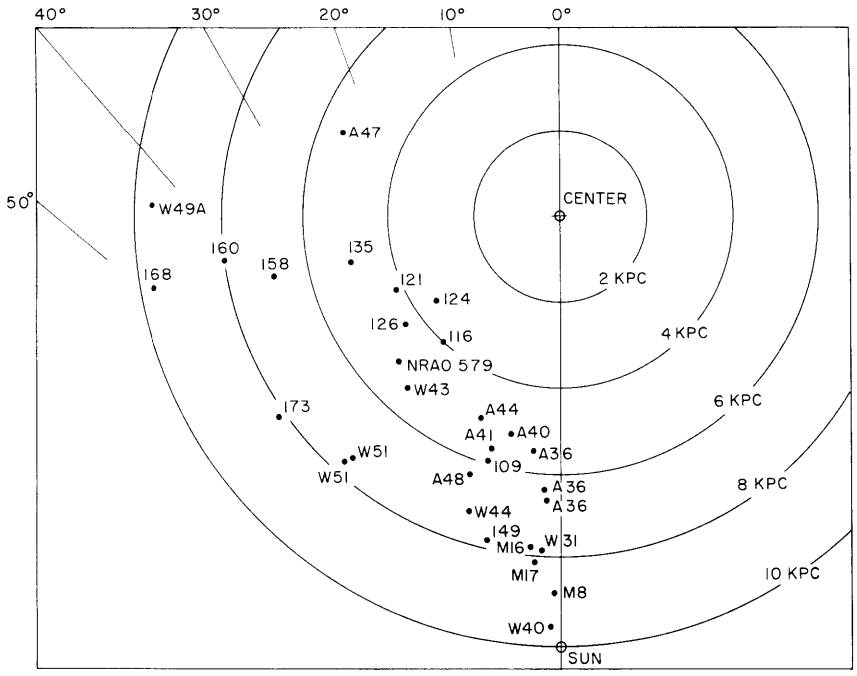

Fig. V-9. Distribution of H II regions in the galaxy.

the galactic plane, we hope to get a better idea of the distribution of very distant H II regions.

Two regions of special interest are Cygnus X and the Galactic Center. We have observed 8 sources in the Galactic Center. Line emission has definitely been found in the sources G 0.5-0.0, G 0.7-0.0 and G 1.1-0.0. The line radial velocities are 46 km/sec, 62 km/sec and -23 km/sec, respectively. These results differ from those in Mezger's Paper II, and after careful study we have concluded that his results are not correct. In particular, Mezger's G 0.2-0.0 line properly belongs to the G 0.7-0.0 component and the G 0.7-0.0 line to the G 1.1-0.0 component. The G 0.7-0.0 component's radial velocity agrees rather well with the OH emission line velocity associated with the source. Line emission has not been found in sources 39, 41, and G 0.0-0.0, G 0.2-0.0 and G 0.9-0.0.

We have observed the 21 sources in Cygnus X listed by Downes and Rinehart,[3] and definitely found the line in 15. The radial velocities range from 10 km/sec to -40 km/sec, with 11 sources having velocities between 4 km/sec and -10 km/sec. Strictly applying the H I velocity-distance relation, one finds 13 sources within 5 kpc of the sun. Since L is nearly 90°, however, the range of radial velocities is small, and any peculiar velocity in the H II regions makes any distance determination difficult. The sources, with their positions and velocities, are shown in Fig. V-10.

There are several interesting features in this region. One is the velocities of DR 17 and DR 18. The velocities exceed the maximum H I velocity in this direction by ~6 km/sec. This may be the peculiar velocity of H II regions in the Cygnus complex,

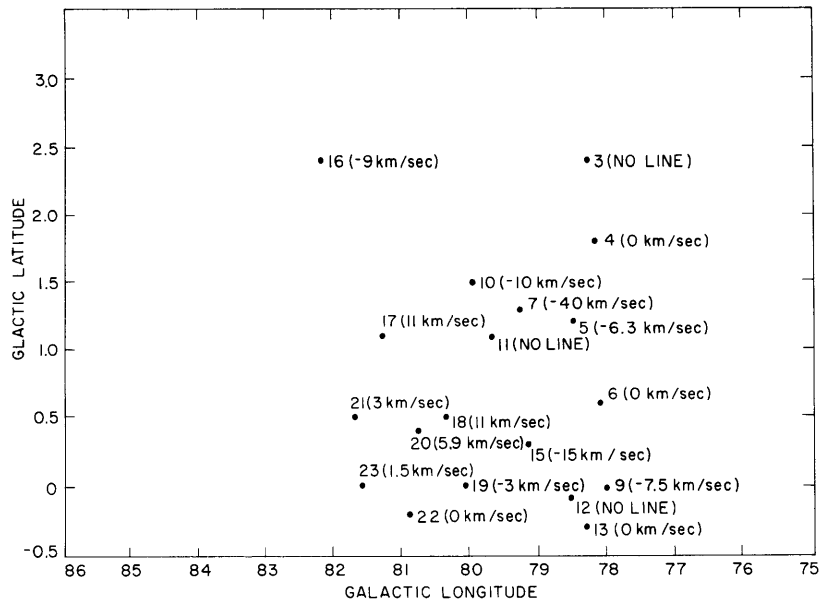

Fig. V-10. Cygnus X sources plotted on the sky, with Hydrogen line VLSR.

or might indicate that HII regions do not follow the HI rotation curve. DR 7 has the highest negative velocity. This might indicate that it is not a member of the group. From the line radial velocity, it is 8 kpc from the sun. DR 4, a source which Downes states is nonthermal, definitely has the line. This line shows that the source has a fairly strong thermal component.

For a reasonable picture of the galaxy in H II, we need a sample that includes many weak sources, particularly between L = 20° and L = 60°. We plan to carry this out in the next observing period. We should then be able to make a meaningful model of the galaxy in the H-109 alpha line and compare this with the H I line matter distribution.

E. C. Reifenstein, T. L. Wilson, B. F. Burke

References

1. P. G. Mezger, and B. Hoglund, Astrophys. J. 147, 490 (1967).
2. A. Glaauw and M. Schmidt (eds.) Stars and Stellar Systems, Vol. V (University of Chicago Press, Chicago, Ill., 1966).
3. D. Downes and R. Rinehart, Astrophys. J. 144, 937 (1966).

F. FLUX OF THE RADIO SOURCE W49 AT 7.83 GHz

The radio source W49 consists of at least 2 components, one thermal, W49A, the other nonthermal, W49B. The thermal source has a spectrum that indicates further structure, a part of which may have high emission measure. In order to determine the flux of the thermal source at 7.83 GHz, observations of W49 were made with the Haystack antenna of Lincoln Laboratory, M.I.T., using a maser radiometer having a system temperature of 70°K. A map of the entire region and an on-off measurement of the thermal source W49A were made. This measurement was referred to W75, which, in turn, was referred to Virgo A, the final standard. This was necessary because Virgo A was not above the horizon when we made the W49 measurement.

Table V-2. Results of measurement.

(1)	(2)	(3)	(4)	(5)	(6)
	T peak	Apparent Source Width	Source Size Correction	T corr.	Flux
W49	5.25°K	.088° × .080°	1.35	7.32°K	64.6
W49B	1.36°K	.088° × .089°	1.46	2.07°K	18.3
W75	2.50°K	.074° × .072°	1.02	2.63°K	23.2
Virgo A	5.32°K	.074° × .072°	1.02	5.64°K	49.7*

*Taken as known (Baars, Mezger, Wendker,[1]).

The measured peak temperatures are in column (2), the apparent source half-widths in (3), and the source size corrections in (4) of Table V-2.

B. F. Burke, T. L. Wilson

References

1. J. W. M. Baars, P. G. Mezger, and H. Wendker (to appear in Astrophys. J.).

G. 1.75-cm INTERFEROMETER

A 1.75-cm interferometer is in the process of construction. The two 8-ft dishes will be placed on the roofs of Buildings 6 and 8, M.I.T. The data will be processed by a small computer, PDP-8. The equipment intended to phase-lock the local oscillator is almost completed, and the rest of the electronic equipment is under way.

B. F. Burke, G. D. Papadopoulos

H. COSMIC BACKGROUND MEASUREMENT

A program has been undertaken to measure the cosmic background radiation at 9.2-mm wavelength. Previous measurements at longer wavelengths indicate that this radiation is characterized by a temperature of approximately 3°K.

The apparatus uses a liquid-helium cooled reference load in a doubly-switched Dicke radiometer. Particular attention has been paid to the symmetry of the first switching stage, in an effort to make an absolute measurement that is accurate to a few tenths of a degree.

Present plans call for a trip this summer to White Mountain, California, to perform the experiment. At this location, the atmospheric brightness temperature should be reduced to less than 5°K. The atmospheric contribution will be determined by means of tilting the radiometer, in addition to some theoretical calculations based on atmospheric models.

B. F. Burke, D. H. Staelin, M. S. Ewing